NUMERICAL APPROXIMATION OF DISCONTINUOUS SOLUTIONS OF THE SEMILINEAR WAVE EQUATION

JIACHUAN CAO*, BUYANG LI* , YANPING LIN* , AND FANGYAN YAO*

Abstract. A high-frequency recovered fully discrete low-regularity integrator is constructed to approximate rough and possibly discontinuous solutions of the semilinear wave equation. The proposed method, with high-frequency recovery techniques, can capture the discontinuities of the solutions correctly without spurious oscillations and approximate rough and discontinuous solutions with a higher convergence rate than pre-existing methods. Rigorous analysis is presented for the convergence rates of the proposed method in approximating solutions such that $(u, \partial_t u) \in C([0, T]; H^\gamma \times H^{\gamma-1})$ for $\gamma \in (0, 1]$. For discontinuous solutions of bounded variation in one dimension (which allow jump discontinuities), the proposed method is proved to have almost first-order convergence under the step size condition $\tau \sim N^{-1}$, where τ and N denote the time step size and the number of Fourier terms in the space discretization, respectively. Numerical examples are presented in both one and two dimensions to illustrate the advantages of the proposed method in improving the accuracy in approximating rough and discontinuous solutions of the semilinear wave equation. The numerical results are consistent with the theoretical results and show the efficiency of the proposed method.

Key words. Semilinear wave equation, discontinuous solution, low regularity, numerical approximation, high/low frequency decomposition, error estimates

AMS subject classifications. 65M12, 65M15, 76D05

1. Introduction. This article concerns the construction and analysis of numerical methods for approximating rough and possibly discontinuous solutions of the semilinear wave equation

$$
\begin{cases}
\partial_{tt} u - \Delta u = g(u) & \text{in } (0, T] \times \Omega \\
u|_{t=0} = u^0 \text{ and } \partial_t u|_{t=0} = v^0 & \text{in } \Omega
\end{cases}
\tag{1.1}
$$

in a domain $\Omega = [0, 1]^d$ with the periodic boundary condition (i.e., Ω is regarded as a d-dimensional torus), where $g : \mathbb{R} \to \mathbb{R}$ is a given nonlinear function. For example, equation (1.1) is often referred to as the sine–Gordon equation when $g(u) = \sin(u)$, and often referred to as the nonlinear Klein–Gordon equation when $g(u) = -mu - \lambda u^3$; see [13, 14, 23]. Since the waves described by the semilinear wave equation propagate with finite speed, the problem in the whole space with compactly supported initial values can also be reduced to a bounded rectangular domain (with periodic boundary condition) which contains the support of the solution on the whole time interval $[0, T]$.

As the relativistic version of the Schrödinger equation, the semilinear wave equation has been wildly used in many physical areas such as quantum field theory, nonlinear optics, dislocated crystals, etc. During the last few decades, the numerical approaches for solving the semilinear wave equation have been extensively investigated, such as trigonometric/exponential integrators that are based on the variation-of-constants formula (for example, see [7, 22, 28, 17, 52]), splitting methods (for example, see [2, 3, 7, 21, 16, 46]), symplectic methods [11, 12, 25], and finite difference methods (such as the Crank–Nicolson, Runge–Kutta and Newmark methods, see [10, 27, 33, 37, 39, 40, 45, 49, 51]). These classical numerical methods have been shown convergent with optimal order to the sufficiently smooth solutions of the semilinear wave equation. However, due to the dispersion feature of (1.1), roughness of the solution may be brought in by randomness or discontinuity of the initial data. This would cause significant challenges in constructing convergent numerical

---

*Department of Applied Mathematics, The Hong Kong Polytechnic University, Hung Hom, Hong Kong. Email address: jiachuan.cao@polyu.edu.hk, buyang.li@polyu.edu.hk, yanping.lin@polyu.edu.hk, fangyan.yao@polyu.edu.hk.

methods for approximating rough solutions, possibly discontinuous and with unbounded energy, of the semilinear wave equation.

Many recent efforts were devoted to the construction and analysis of low-regularity integrators for nonlinear dispersive equations, such as the KdV equation [29, 54, 56, 57] and the nonlinear Schrödinger equation [6, 41, 42, 48]. In these articles, several different approaches have been developed for constructing numerical methods that are convergent under low-regularity conditions, with higher-order convergence than the classical methods, including the resonance-based approach which uses variation-of-constants formulae and twisted variables [6, 29, 41, 44, 54, 55, 56, 57], the semigroup based technique using the cancellation structures in the solution representations [48, 34], and low-regularity integrators based on discrete Bourgain/Strichartz estimates [42]. Recently, based on new schemes to approximate the nonlinear frequency interaction and a new harmonic analysis technique by using the Littlewood-Paley dyadic decomposition, first-order low-regularity schemes for the cubic nonlinear Schrödinger equation were introduced in [36] and [1] to allow almost first-order convergence in the L^2 norm for H^1 initial data with periodic and Neumann boundary conditions respectively. Moreover, based on a temporal averaging technique and more careful high order resonance analysis, a new second-order scheme was proposed in [8], which can have second-order convergence in the L^2 norm with initial data strictly below H^2. These newly developed approaches have significantly improved the convergence rates of numerical solutions to these nonlinear dispersive equations under low regularity conditions.

Low regularity integrators for the semilinear wave equation was addressed by Rousset & Schratz in [48] by using transformation $w = u - i(-\Delta)^{-\frac{1}{2}}\partial_t u$, which converts the semilinear wave equation into a first-order formulation, i.e.,

$$i\partial_t w = -(-\Delta)^{\frac{1}{2}}w + (-\Delta)^{-\frac{1}{2}}g\Big(\frac{w + \bar{w}}{2}\Big). \qquad (1.2)$$

They constructed a low-regularity integrator for the first-order equation in (1.2) with second-order convergence in the energy norm $H^1 \times L^2$ under the regularity condition $(u^0, v^0) \in H^{\frac{7}{4}} \times H^{\frac{3}{4}}$ in three dimensions.

A different low-regularity integrator for (1.1) was constructed in [35] directly based on the discovery of a new cancellation structure, also with second-order convergence in $H^1 \times L^2$ under the regularity condition $(u^0, v^0) \in H^{1+\frac{d}{4}} \times H^{\frac{d}{4}}$ for spatial dimension $d = 1, 2, 3$. For the nonlinear term $g(u) = mu + \lambda u^3$ with given constants $m \geq 0$ and $\lambda \in \mathbb{R}$, a symmetric low-regularity integrator was constructed in [53] for the semilinear Klein–Gordon equation on a one-dimensional torus, with second-order convergence in $H^\gamma \times H^{\gamma-1}$ under the condition $(u^0, v^0) \in H^\gamma \times H^{\gamma-1}$ for $\gamma > \frac{1}{2}$.

These low-regularity integrators all require the solution $(u, \partial_t u)$ to be in $H^\gamma \times H^{\gamma-1}$ with $\gamma > \frac{d}{2}$, thus requiring the solution u to be continuous. However, the semilinear wave equation can be well-posed even for discontinuous solutions below the energy space. For example, the sine–Gordon equation is well-posed in $H^\gamma \times H^{\gamma-1}$ for all $\gamma \geq 0$ and the semilinear Klein–Gordon equation is well-posed in $H^\gamma \times H^{\gamma-1}$ for $\gamma > \frac{1}{3}$ in the one dimensional case [5], and for $\gamma \geq 1$ in the high dimensional cases [19, 20]. The construction and analysis of convergent numerical methods for approximating such rough and discontinuous solutions of the semilinear wave equation are still interesting and challenging.

The aim of this paper is to construct a more efficient fully discrete low-regularity integrator for approximating possibly discontinuous solutions of the semilinear wave equation in one and two dimensions. To improve the convergence rates of numerical solutions in approximating rough solutions, we design a numerical scheme which could approximate the low-frequency and high-frequency parts of the solution separately, by approximating the low-frequency part with a time-stepping scheme and the high-frequency part with a recovery technique. The high-frequency recovery, which has equivalent computational cost as the approximation to the low-frequency part, could significantly improve the accuracy of the numerical solutions and therefore could capture the discontinuities in the rough solution

by significantly reducing spurious oscillations. The advantages of the proposed method are demonstrated numerically in Section 7 and proved rigorously in a particular setting, for approximating discontinuous solutions of bounded variation (such as piecewise smooth solutions) in one dimension.

By utilizing the cancellation structure of the semilinear wave equation discovered in [35] and the new techniques developed in this paper, we prove the following error bounds in the $L^2 \times H^{-1}$ norm for approximating a solution $(u, \partial_t u) \in C([0, T]; H^\gamma \times H^{\gamma-1})$:

$$O(N^{-\gamma+} + \tau N^{1-2\gamma+}) \qquad\qquad \text{for } \gamma \in \left(0, \frac{1}{2}\right],$$

$$O\big(N^{-\gamma+} + \tau N^{1-2\gamma+} + \min(\tau, \tau^2 N^{2(1-\gamma)+})\big) \qquad \text{for } \gamma \in \left(\frac{1}{2}, 1\right],$$

where N denotes the number of Fourier terms used in each dimension of the space discretization. Therefore, the error is $O(\tau^\gamma)$ under the step size condition $\tau \sim N^{-1}$, and the convergence rate could be further improved by choosing a different step size condition which depends on the regularity of the solution.

More importantly, we prove that for discontinuous solutions with bounded variation in one dimension (e.g., piecewise smooth solutions with jump discontinuities) the proposed numerical scheme has better convergence rate (i.e., almost first-order convergence) in $L^2 \times H^{-1}$ under the step-size condition $\tau \sim N^{-1}$.

Extensive numerical experiments, including both one- and two-dimensional examples, are given to illustrate the effectiveness (higher-order accuracy and reduction of spurious oscillation) of the proposed method in approximating rough and discontinuous solutions of the semilinear wave equation.

The rest of this article is organized as follows. In Section 2, we introduce some basic notations and present the main theoretical results of this article on the convergence rates of the proposed numerical method. In Section 3 we present some preliminary and technical results have will be used in the construction and analysis of the method. The construction of the numerical scheme is presented in Section 4. The proof of the main theoretical results are presented in Section 5 and Section 6, respectively. Finally, we present extensive numerical examples in Section 7 to support the theoretical results and to illustrate the effectiveness of the proposed method in approximating rough and discontinuous solutions of the semilinear wave equation.

2. Notations and main results. In this section we present the basic notations and main results of this paper, including the proposed numerical scheme and the convergence of the numerical approximations to rough solutions of the semilinear wave equation.

2.1. Notations and numerical scheme. We rewrite the second-order semilinear wave equation in (1.1) into a first-order system of equations, i.e.,

$$\begin{cases} \partial_t U - LU = F(U) \text{ in } (0, T] \times \Omega, \\ U(0) = U^0 \text{ in } \Omega, \end{cases} \tag{2.1}$$

with

$$U = \begin{pmatrix} u \\ \partial_t u \end{pmatrix}, \quad U^0 = \begin{pmatrix} u^0 \\ v^0 \end{pmatrix}, \quad F(U) = \begin{pmatrix} 0 \\ f(u) \end{pmatrix}, \quad L = \begin{pmatrix} 0 & 1 \\ \widetilde{\Delta} & 0 \end{pmatrix},$$

where we have used the following notations:

$$f(u) = g(u) + mu \quad \text{and} \quad \widetilde{\Delta} = \Delta - m \text{ with some fixed constant } m > 0.$$

The fixed constant $m > 0$ is introduced to make sure that the linear operator L is reversible on the d-dimensional torus $\Omega = [0, 1]^d$.

We denote by e^{tL} the solution operator of the linear wave equation (i.e., the map from U^0 to $U(t)$ in the case $F(U) \equiv 0$). By defining the a-norm of a function $W = (w_1, w_2)^T \in$

3

$H^a(\Omega) \times H^{a-1}(\Omega)$, i.e.,

$$\|W\|_a = (\|w_1\|_{H^a}^2 + \|w_2\|_{H^{a-1}}^2)^{\frac{1}{2}}, \quad a \in \mathbb{R}.$$

the following properties hold:

$$\|e^{tL}W\|_0 \lesssim \|W\|_0, \quad \|e^{tL}W\|_1 \lesssim \|W\|_1, \tag{2.2}$$

$$\|F(U)\|_1 \lesssim \|f(u)\|_{L^2} \lesssim f(0) + \|f'\|_{L^\infty}\|U\|_0. \tag{2.3}$$

It is known that any function in the Sobolev space $L^2(\Omega)$ can be expanded into a Fourier series. Accordingly, we introduce the finite-dimensional subspace

$$S_N = \Big\{ \sum_{n_1,\cdots,n_d=-N}^{N} c_{n_1,\cdots,n_d} \exp\left(2n_1\pi x_1 i\right) \cdots \exp\left(2n_d\pi x_d i\right) : c_{n_1,\cdots,n_d} \in \mathbb{C} \Big\},$$

and approximate functions in $H^s(\Omega)$ by using the finite-dimensional subspace S_N. We denote by Π_N the L^2 projection operator onto S_N defined by

$$(w - \Pi_N w, v) = 0, \quad \forall v \in S_N, \quad w \in H^s(\Omega),$$

and denote $\Pi_{>N} := I - \Pi_N$ and $\Pi_{(N_1,N_2]} := \Pi_{N_2} - \Pi_{N_1}$ for $N_2 > N_1$. We denote by $I_N : H^s \to S_N$ the trigonometric interpolation such that for any function $w \in H^s$, $s > \frac{d}{2}$, $(I_N w)(x) = w(x)$ for $x \in D^d$, with

$$D = \Big\{ \frac{n}{2N} : n = 0, \cdots, 2N-1 \Big\}.$$

We define the sequence of grid points $t_n = n\tau$, $n = 0, 1, \ldots, M$, in the time interval $[0, T]$ with step size $\tau = T/M$, and denote by $U^n = (u^n, v^n)^T$ the numerical solution at time $t = t_n$. Then the high-frequency recovering low-regularity integrator for the equation (2.1) constructed in this article reads (the detailed construction is presented in Section 4):

$$U_N^{n+1} = \Pi_N U_N^{n+1} + \Pi_{(N,N^\alpha]} U_N^{n+1}, \tag{2.4a}$$

$$\Pi_N U_N^{n+1} = e^{\tau L}\Pi_N U_N^n + \tau e^{\tau L}I_N F(\Pi_N U_N^n)$$
$$+ (2L)^{-1}\left[\tau e^{\tau L} - (2L)^{-1}(e^{\tau L} - e^{-\tau L})H(\Pi_N U_N^n)\right], \tag{2.4b}$$

$$\Pi_{(N,N^\alpha]} U_N^{n+1} = e^{(n+1)\tau L}\Pi_{(N,N^\alpha]} U_N^0, \tag{2.4c}$$

with

$$H(U) = \begin{pmatrix} -I_N f(u) \\ \Pi_N(I_N f'(u) \cdot v) \end{pmatrix}, \tag{2.5}$$

and initial value $U_N^0 = \Pi_{N^\alpha}U(0)$ for $\alpha \geq 1$. This scheme introduces an additional high-frequency part to the low-regularity integrator in [35], and uses a different definition of $H(U)$ to obtain the desired convergence rates for approximating discontinuous solutions. It is the combination of the filtered low-regularity integrator (2.4b) and high-frequency recovery process (2.4c), ensures the accuracy of the proposed method for approximating rough solutions under lower-regularity conditions than [35].

REMARK 2.1. In (2.4) we see that the high- and low-frequency parts of U_N^{n+1} are computed separately, independent of each other, where the low-frequency part is computed by a time-stepping scheme and the high-frequency part is recovered directly from its initial value via (2.4c) (without time steppings). Since the nonlinear terms in (2.4b) can be computed by using the Fast Fourier Transform (FFT), the computational cost at every time level is $O(N^d \log(N))$. Therefore, the total cost for computing the low-frequency part at time T is $O(N^d \log(N)T/\tau)$. In contrast, the high-frequency part of the numerical solution needs not be computed every time level. Instead, we only need to compute (2.4c) once to recover the high-frequency part of U_N^{n+1} for any particular time level of interest. Therefore, the cost of computing the high-frequency part at time T is $O(N^{\alpha d})$, which is comparable to the cost of computing the low-frequency part if we choose $N^{(\alpha-1)d} \sim T/\tau$.

Under the step size condition $\tau \sim N^{-1}$, this suggests to choose $\alpha = 1 + \frac{1}{d}$ in the computation. The advantages of this choice is analyzed rigorously in Theorem 2.2 in one dimension and illustrated numerically in Section 7 in both one and two dimensions.

REMARK 2.2. *The trigonometric interpolation operator I_N is used in (2.4b) and (2.5) to approximate nonlinear functions by Fourier series using FFT. This makes the algorithm more efficient than using the projection operator Π_N, but also increases the difficulty of convergence analysis under low-regularity conditions.*

2.2. Main theoretical results. For the simplicity of notation, we denote by $A \lesssim B$ or $B \gtrsim A$ the statement $A \leq CB$ for some constant $C > 0$. The value of C may depend on T and $\|U\|_\gamma$, and may be different at different occurrences, but is always independent of step size τ, degrees of freedom N (in each dimension), and time level n. The notation $A \sim B$ means that $A \lesssim B \lesssim A$. If a statement contains $s+$ or $s-$ for some number s, it means that the statement holds with $s + \epsilon$ or $s - \epsilon$ for arbitrary $\epsilon > 0$; see Theorem 2.1.

The convergence of the proposed algorithm in (2.4) in the general setting is presented in the following theorem.

THEOREM 2.1. *Let $d = 1, 2$ and $\gamma \in (0, 1]$, and assume that the nonlinear function $f : \mathbb{R} \to \mathbb{R}$ satisfies the following condition:*

$$|f'(s)| + |f''(s)| + |f'''(s)| \lesssim 1. \tag{2.6}$$

Then, under the regularity condition $U \in C([0, T]; H^\gamma(\Omega) \times H^{\gamma-1}(\Omega))$ and the step size condition $N \lesssim \tau^{-\frac{1}{1-\gamma}+\epsilon_0}$ (for an abitrary $\epsilon_0 \in (0, 1]$), the numerical solutions given by (2.4) for each $\alpha \geq 1$ converge to the solution of (2.1) with the following error estimates.

(i) For $\gamma \in (0, \frac{1}{2}]$, there exist constants $\tau_0 \in (0, 1)$ and $C_0 > 0$ such that, for step size $\tau \in (0, \tau_0]$,

$$\max_{0 \leq n \leq T/\tau} \|U(t_n) - U_N^n\|_0 \leq C_0(N^{-\gamma+} + \tau N^{1-2\gamma+}). \tag{2.7}$$

(ii) For $\gamma \in (\frac{1}{2}, 1]$, there exist constants $\tau_0 \in (0, 1)$ and $C_0 > 0$ such that, for step size $\tau \in (0, \tau_0]$,

$$\max_{0 \leq n \leq T/\tau} \|U(t_n) - U_N^n\|_0 \leq C_0(N^{-\gamma+} + \tau N^{1-2\gamma+} + \min(\tau, \tau^2 N^{2(1-\gamma)+})). \tag{2.8}$$

The constants C_0 and τ_0 may depend on ϵ_0 in the condition $N \lesssim \tau^{-\frac{1}{1-\gamma}+\epsilon_0}$ (when ϵ_0 is smaller, τ_0 is smaller and C_0 is bigger).

REMARK 2.3. *Under the condition (2.6), by constructing a contraction map, standard techniques can be used to prove that problem (2.1) admits a unique solution $U = (u, \partial_t u) \in L^\infty(0, T; H^\gamma \times H^{\gamma-1})$. This solution is automatically in $C([0, T]; H^\gamma \times H^{\gamma-1})$.*

REMARK 2.4. *The theoretical error estimates in Theorem 2.1 implies that, by choosing $\tau \sim N^{-1}$ (independent of the regularity of the initial data) and $\alpha = 1$ (without high-frequency recovery), the errors of the numerical solutions is bounded by $O(\tau^{\gamma-})$ for approximating solutions in $H^\gamma(\Omega) \times H^{\gamma-1}(\Omega)$ with $\gamma \in (0, 1]$. However, in practical computation, the errors of the numerical solutions can often be significantly reduced by using high-frequency recovery with $\alpha = 1 + \frac{1}{d}$ under the step size condition $\tau \sim N^{-1}$ with equivalent computational cost; see Remark 2.1. Such advantages of the high-frequency recovery technique proposed in (2.4) is demonstrated numerically in Section 7 and proved rigorously in the following theorem in a particular setting, for approximating discontinuous solutions of bounded variation (such as piecewise smooth solutions) in one dimension.*

Let $BV(\Omega)$ denote the set of functions with bounded variations on Ω with norm $\|u\|_{BV} := \|u\|_{L^1} + \|\nabla u\|_M$, where M denotes the norm of $M(\Omega)$, the space of Borel measures on Ω (the norm of $M(\Omega)$ is equivalent to the L^1 norm for integrable functions).

THEOREM 2.2. *Let $d = 1$ (i.e., consider the one-dimensional problem) and assume that the solution has the following regularity:*

$$(u, \partial_t u) \in C([0, T]; H^{\frac{1}{2}-}(\Omega) \times H^{-\frac{1}{2}-}(\Omega)) \quad and \quad u \in L^\infty(0, T; BV(\Omega) \cap L^\infty(\Omega)).$$

Then, under the step size condition $\tau \sim N^{-1}$, the numerical solutions given by (2.4) with $\alpha = 2$ converge to the solution of the continuous problem in (2.1) with the following rate:

$$\max_{0 \leq n \leq T/\tau} \|U(t_n) - U_N^n\|_0 \lesssim \tau^{1-}. \tag{2.9}$$

REMARK 2.5. For an initial value in $(u_0, v_0) \in BV(\Omega) \times M(\Omega)$, the additional regularity condition $u \in L^\infty(0, T; BV(\Omega) \cap L^\infty(\Omega))$ in Theorem 2.2 naturally holds for the one-dimensional sine-Gordon equation

$$\begin{cases} \partial_{tt} u - \partial_{xx} u = \sin(u) & \text{in } (0, T] \times \Omega \\ u|_{t=0} = u_0, \quad \partial_t u|_{t=0} = v_0 & \text{on } \Omega. \end{cases} \tag{2.10}$$

For example, we consider (2.10) with initial value $u_0 \in BV(\Omega)$ on the interval $\Omega = [0, 1]$ with the periodic boundary condition. Let $\tilde{u}$, $\tilde{u}_0$ and $\tilde{v}_0$ be the periodic extensions of u, u_0 and v_0 to $\mathbb{R}$, respectively. Then d'Alambert's formula and Duhamel's formula imply that

$$\tilde{u}(t, x) = \frac{1}{2} \int_0^t \int_{x-t+s}^{x+t-s} \sin(\tilde{u})(s, y) dy ds + \frac{1}{2} (\tilde{u}_0(x+t) + \tilde{u}_0(x-t)) + \frac{1}{2} \int_{x-t}^{x+t} \tilde{v}_0(y) dy. \tag{2.11}$$

By taking the BV and L^∞ norm on both sides of (2.11) and then summing up the two results, we can see that $u(t) \in BV(\Omega)$ for all $t \in [0, T]$ and

$$\|u(t)\|_{BV} + \|u(t)\|_{L^\infty} \lesssim T^2 + \|u_0\|_{BV} + \|u_0\|_{L^\infty} + \|v_0\|_M.$$

This shows that the regularity condition in Theorem 2.2 naturally characterizes the regularity of the solutions with discontinuous initial data in $BV(\Omega)$.

REMARK 2.6. Without the high-frequency recovery, the convergence rate of the proposed method would reduce to half order from first order. This can be seen from the proof of Theorem 2.2 and can also be observed in the numerical tests.

REMARK 2.7. From the numerical examples in Section 7.2 we can see that the high-frequency recovery in (2.4), with $\alpha = \frac{3}{2}$ under the step size condition $\tau \sim N^{-1}$, also improves the convergence rates in approximating discontinuous solutions from half to $\frac{3}{4}$ in two dimensions.

3. Preliminary results. In this section we present some preliminary results to be used in the proofs of Theorem 2.1 and Corollary 2.2. These include Bernstein's inequalities in the L^p norm (Lemma 3.1), approximation properties of the trigonometric interpolation (Lemma 3.2), L^p error of trigonometric interpolation (Lemma 3.3), and negative-norm estimates for the product of two functions (Lemma 3.4 and Lemma 3.5). The proof of Lemma 3.3 and Lemma 3.4 can be found in the arXiv version of this paper [9], which contains the complete proofs of some technical lemmas.

LEMMA 3.1 (Bernstein's inequality; cf. [24, Theorem 2.2 and pp. 22]). *Let f be a function such that $J^\gamma f := (1 - \Delta)^{\frac{\gamma}{2}} f \in L^p(\Omega)$ for some $\gamma \geq 0$ and $1 < p < \infty$. Then the following results hold:*

$$\|\Pi_{\leq N} J^\gamma f\|_{L^p} \lesssim N^\gamma \|f\|_{L^p}, \qquad \|\Pi_{>N} f\|_{L^p} \lesssim N^{-\gamma} \|J^\gamma f\|_{L^p}.$$

LEMMA 3.2 (Standard error of trigonometric interpolation; cf. [32, Theorem 11.8]). *Let f be a function such that $f \in H^\gamma(\Omega)$. For $0 \leq s \leq \gamma$ and $\gamma > \frac{d}{2}$, we have*

$$\|f - I_N f\|_{H^s} \lesssim N^{-(\gamma-s)} \|f\|_{H^\gamma}.$$

LEMMA 3.3 (Error of trigonometric interpolation in the L^p norm; see [9]). *Let $d = 1$ and $f \in W^{1,p}(\Omega)$ for $1 < p < \infty$ then*

$$\|f - I_N f\|_{L^p} \lesssim N^{-1} \|f\|_{W^{1,p}}.$$

LEMMA 3.4 (Negative-norm estimates for the product of two functions; see [9]). *For $d = 1, 2$, the following estimates hold:*

$$\|fg\|_{H^{-1}} \lesssim \|g\|_{H^{-1}} \left(\|f\|_{L^\infty} + \|f\|_{H^{1+}} \right), \tag{3.1}$$

$$\|fg\|_{H^{-1}} \lesssim \|f\|_{L^{2+}}^\gamma \|f\|_{H^{1+}}^{1-\gamma} \|g\|_{H^{\gamma-1}}, \tag{3.2}$$

$$\|fg\|_{H^{-1}} \lesssim \|f\|_{L^2}\|g\|_{L^{2+}}. \tag{3.3}$$

In addition, for any $\gamma \in (0,1]$ and function $h \in L^\infty$, the following estimate holds:

$$\|fgh\|_{H^{\gamma-1}} \lesssim \|f\|_{L^2}\|g\|_{H^{\gamma+}}\|h\|_{L^\infty}. \tag{3.4}$$

LEMMA 3.5. *Let* $(u,v)^T \in H^\gamma(\Omega) \times H^{\gamma-1}(\Omega)$ *and assume that f satisfies the conditions in* (2.6). *Then the following estimates hold:*

$$\|f'(\Pi_N u)\Pi_N v\|_{H^{-1}} \lesssim N^{1-2\gamma+} \qquad for \quad \gamma \in (0, \tfrac{1}{2}], \tag{3.5}$$

$$\|f'(\Pi_N u)\Pi_N v\|_{H^{-1}} \lesssim 1 \qquad for \quad \gamma \in (\tfrac{1}{2}, 1]. \tag{3.6}$$

Proof. Without loss of generality, we assume that $\log_2 N$ is an integer (otherwise we replace $\log_2 N$ by the smallest integer larger than it). Then, by using the triangle inequality, we have

$$\|f'(\Pi_N u) \cdot \Pi_N v\|_{H^{-1}} \leq \sum_{k=1}^{\log_2 N - 1} \|(f'(\Pi_{2^{k+1}}u) - f'(\Pi_{2^k}u))\Pi_N v\|_{H^{-1}}. \tag{3.7}$$

The right-hand side of (3.7) can be estimated by using (3.2), i.e.,

$$\|(f'(\Pi_{2^{k+1}}u) - f'(\Pi_{2^k}u))\Pi_N v\|_{H^{-1}}$$

$$\lesssim \|f'(\Pi_{2^{k+1}}u) - f'(\Pi_{2^k}u)\|_{L^{2+}}^\gamma \|f'(\Pi_{2^{k+1}}u) - f'(\Pi_{2^k}u)\|_{H^{1+}}^{1-\gamma}\|\Pi_N v\|_{H^{\gamma-1}}$$

$$\lesssim \|f''\|_{L^\infty}^\gamma \|\Pi_{2^{k+1}}u - \Pi_{2^k}u\|_{L^{2+}}^\gamma \cdot (\|f'(\Pi_{2^{k+1}}u)\|_{H^{1+}} + \|f'(\Pi_{2^k}u)\|_{H^{1+}})^{1-\gamma}\|\Pi_N v\|_{H^{\gamma-1}}$$

$$\lesssim [(2^k)^{-\gamma+}]^\gamma [(2^k)^{1-\gamma+}]^{1-\gamma} \lesssim (2^k)^{1-2\gamma+},$$

here in the third inequality, we have used the boundedness of $\|f''\|_{L^\infty}$ and $\|\Pi_N v\|_{H^{\gamma-1}}$, and the following estimates:

$$\|\Pi_{2^{k+1}}u - \Pi_{2^k}u\|_{L^{2+}} \lesssim \|\Pi_{2^{k+1}}u - \Pi_{2^k}u\|_{L^2}^{1-} \|\Pi_{2^{k+1}}u - \Pi_{2^k}u\|_{H^1}^{0+}$$

$$\lesssim \left((2^k)^{-\gamma}\|u\|_{H^\gamma}\right)^{1-} \left((2^k)^{1-\gamma}\|u\|_{H^\gamma}\right)^{0+} \lesssim (2^k)^{-\gamma+},$$

and

$$\|f'(\Pi_{2^k}u)\|_{H^{1+}} \lesssim \|f'(\Pi_{2^k}u)\|_{H^1}^{1-} \|f'(\Pi_{2^k}u)\|_{H^2}^{0+}$$

$$\lesssim \left(\|f'\|_{L^\infty} + \|f''\|_{L^\infty}\|\Pi_{2^k}u\|_{H^1}\right)^{1-}$$

$$\cdot \left(\|f'\|_{L^\infty} + \|f''\|_{L^\infty}\|\Pi_{2^k}u\|_{H^2} + \|f'''\|_{L^\infty}\left\|(\Pi_{2^k}\nabla u)^2\right\|_{L^2}\right)^{0+}$$

$$\lesssim \left(1 + (2^k)^{1-\gamma}\|u\|_{H^\gamma}\right)^{1-} \left[1 + (2^k)^{2-\gamma}\|u\|_{H^\gamma} + \left((2^k)^{1+\frac{d}{4}-\gamma}\|u\|_{H^\gamma}\right)^2\right]^{0+}$$

$$\lesssim (2^k)^{1-\gamma+}.$$

For $\gamma \in (0, \tfrac{1}{2}]$, we sum up the above estimate for $k = 1, \ldots, \log_2 N - 1$. This leads to the following result:

$$\|\Pi_N(f'(\Pi_N \tilde{u}) \cdot \Pi_N \tilde{v})\|_{H^{-1}} \lesssim \sum_{k=1}^{\log_2 N - 1} (2^k)^{1-2\gamma+} \lesssim N^{1-2\gamma+} \cdot \log_2 N.$$

This proves the first result of Lemma 3.5, where the term $\log_2 N$ can be absorbed into the $N^{1-2\gamma+}$ with the presence of the "+" in the exponent.

For $\gamma \in (\tfrac{1}{2}, 1]$, we have $1 - 2\gamma+ < 0$ and therefore $\|\Pi_N(f'(\Pi_N \tilde{u}) \cdot \Pi_N \tilde{v})\|_{H^{-1}} \lesssim 1$. This proves the second result of Lemma 3.5. $\square$

Next, we present some useful properties/structures of the vector-valued function $F(U)$ that play important roles in the convergence of the proposed low-regularity integrator for approximating rough solutions below the energy space. Since $F(U) = (0, f(u))^T$, it is

7

straightforward to verify that, for $W = (w_1, w_2)^T$ and $W^* = (w_1^*, w_2^*)^T$,

$$F'(U) = \begin{pmatrix} 0 & 0 \\ f'(u) & 0 \end{pmatrix}, \quad F'(U)W = \begin{pmatrix} 0 \\ f'(u)w_1 \end{pmatrix}, \quad F''(U)W \cdot W^* = \begin{pmatrix} 0 \\ f''(u)w_1 w_1^* \end{pmatrix}.$$
(3.8)

The next lemma is a fundamental ingredient in the construction of the second-order low-regularity integrator proposed in [35].

LEMMA 3.6. *Let $U = (u, v)^T$ and $\tilde{U}(s) := e^{sL}U = (\tilde{u}(s), \tilde{v}(s))^T$. Then the following identities hold*

$$\frac{d}{ds} e^{-sL} F(\tilde{U}(s)) = e^{-sL} \begin{pmatrix} -f(\tilde{u}(s)) \\ f'(\tilde{u}(s)) \cdot \tilde{v}(s) \end{pmatrix},$$
(3.9)

and

$$\frac{d}{ds} \left[e^{2sL} \frac{d}{ds} \left(e^{-sL} F(\tilde{U}(s)) \right) \right] = e^{sL} \begin{pmatrix} 0 \\ f''(\tilde{u}(s))(|\tilde{v}(s)|^2 - |\nabla \tilde{u}(s)|^2) + m(\tilde{u}(s) - f(\tilde{u}(s))) \end{pmatrix}.$$
(3.10)

Moreover,

$$\int_0^\tau e^{(\tau-s)L} F(\tilde{U}(s)) ds = \tau e^{\tau L} F(U) + (2L)^{-1} [\tau e^{\tau L} - (2L)^{-1}(e^{\tau L} - e^{-\tau L})] \begin{pmatrix} -f(u) \\ f'(u)v \end{pmatrix}$$

$$+ \int_0^\tau e^{(\tau-2s)L}(\tau - s) \int_0^s \frac{d}{d\sigma} \left[e^{2\sigma L} \frac{d}{d\sigma} \left(e^{-\sigma L} F(\tilde{U}(\sigma)) \right) \right] d\sigma ds.$$
(3.11)

Equation (3.10) is the cancellation structure in the semilinear wave equation discovered by [35]. This cancellation structure ensures that all spatial second-order derivatives on the right-hand side of (3.10) are canceled out, allowing us to construct suitable numerical approximations for the nonlinear term using Equation (3.11), while avoiding higher-order derivative terms in the error analysis. The proof of the above lemma involves the application of the chain rule, the Fubini theorem, and integration by parts. For detailed proofs and further information, refer to [35, (2.23) and (2.26)]. Furthermore, the following result, which can be found in [35, (2.44)] will be useful later,

$$\left\| \frac{d}{d\sigma} e^{-\sigma L} \left[F'(\tilde{U}(\sigma)) e^{\sigma L} W \right] \right\|_1 \lesssim \|W\|_{\frac{3}{2}+\epsilon} \|\tilde{U}(\sigma)\|_1 + \|W\|_1.$$
(3.12)

4. Construction of the numerical scheme. In this section, we demonstrate the construction of the high frequency recovered low-regularity integrator in (2.4). We start with the variation-of-constants formula, i.e.,

$$U(t_{n+1}) = e^{\tau L} U(t_n) + \int_0^\tau e^{(\tau-s)L} F(U(t_n + s)) ds$$
(4.1)

and employ the following high- and low-frequency decomposition:

$$U(t_{n+1}) = e^{\tau L} U(t_n) + \int_0^\tau e^{(\tau-s)L} \Pi_N F(\Pi_N U(t_n + s)) ds + R_1(t_n),$$
(4.2)

where the remainder $R_1(t_n)$ is given by

$$R_1(t_n) = \int_0^\tau e^{(\tau-s)L} \left[F(U(t_n + s)) - \Pi_N F(\Pi_N U(t_n + s)) \right] ds.$$
(4.3)

Then we approximate the low-frequency term.

Since Π_N commutes with L, by using the Taylor expansion of $F(U)$ at $U = e^{sL} \Pi_N U(t_n)$, we have

$$F(\Pi_N U(t_n + s)) = F(e^{sL} \Pi_N U(t_n)) + F'(e^{sL} \Pi_N U(t_n)) \int_0^s e^{(s-\sigma)L} \Pi_N F(\Pi_N U(t_n + \sigma)) d\sigma$$

$$+ \tilde{R}_2(s) + \tilde{R}_3(s),$$

8

where

$$\tilde{R}_2(s) = F'(e^{sL}\Pi_N U(t_n)) \int_0^s e^{(s-\sigma)L}\Pi_N\Big[F(U(t_n+\sigma)) - F(\Pi_N U(t_n+\sigma))\Big]d\sigma, \qquad (4.4)$$

$$\tilde{R}_3(s) = R_F(s)\int_0^s e^{(s-\sigma)L}\Pi_N F(U(t_n+\sigma))d\sigma \cdot \int_0^s e^{(s-\sigma)L}\Pi_N F(U(t_n+\sigma))d\sigma, \qquad (4.5)$$

$$R_F(s) = \int_0^1\int_0^1 \theta F''\left[(1-\sigma)e^{sL}\Pi_N U(t_n) + \sigma(1-\theta)e^{sL}\Pi_N U(t_n) + \theta\sigma\Pi_N U(t_n+s)\right]d\sigma d\theta.$$

Inserting the above results to (4.2), we obtain

$$U(t_{n+1}) = e^{\tau L}U(t_n) + I_1(t_n) + I_2(t_n) + R_1(t_n) + R_2(t_n) + R_3(t_n),$$

where

$$I_1(t_n) = \int_0^\tau e^{(\tau-s)L}\Pi_N F(\Pi_N\tilde{U}(t_n+s))ds, \quad \tilde{U}(t_n+s) = e^{sL}U(t_n), \qquad (4.6)$$

$$I_2(t_n) = \int_0^\tau e^{(\tau-s)L}\Pi_N\left[F'(\Pi_N\tilde{U}(t_n+s))\int_0^s e^{(s-\sigma)L}\Pi_N F(\Pi_N U(t_n+\sigma))d\sigma\right]ds,$$

$$R_2(t_n) = \int_0^\tau e^{(\tau-s)L}\Pi_N\tilde{R}_2(s)ds, \quad R_3(t_n) = \int_0^\tau e^{(\tau-s)L}\Pi_N\tilde{R}_3(s)ds. \qquad (4.7)$$

The approximation of $I_1(t_n)$ combines the filtering technique and Lemma 3.6. Using (3.11) with $U = \Pi_N U(t_n)$ and interchanging Π_N and L in order, we obtain

$$I_1(t_n) = \tau e^{\tau L}\Pi_N F(\Pi_N U(t_n))$$
$$+ (2L)^{-1}\left[\tau e^{\tau L} - (2L)^{-1}(e^{\tau L} - e^{-\tau L})\right]\begin{pmatrix} -\Pi_N f(\Pi_N u(t_n)) \\ \Pi_N(f'(\Pi_N u(t_n))\Pi_N v(t_n)) \end{pmatrix} + R_4(t_n),$$

where

$$R_4(t_n) = \int_0^\tau e^{(\tau-2s)L}(\tau-s)\int_0^s \frac{d}{d\sigma}\left[e^{2\sigma L}\frac{d}{d\sigma}e^{-\sigma L}\Pi_N F(\Pi_N\tilde{U}(t_n+\sigma))\right]d\sigma ds. \qquad (4.8)$$

For $I_2(t_n)$, by approximating $\Pi_N U(t_n+\sigma)$ with $\Pi_N e^{\sigma L}U(t_n)$, we obtain

$$I_2(t_n) = \int_0^\tau e^{(\tau-s)L}\Pi_N\left[F'(\Pi_N\tilde{U}(t_n+s))\int_0^s e^{(s-\sigma)L}\Pi_N F(\Pi_N U(t_n+\sigma))d\sigma\right]ds \qquad (4.9)$$

$$= \int_0^\tau se^{\tau L}\Pi_N\left[F'(\Pi_N U(t_n))\Pi_N F(\Pi_N U(t_n))\right]ds + R_5(t_n) + R_6(t_n) + R_7(t_n), \qquad (4.10)$$

where the first term is equal to 0 due to (3.8) and the remaining terms are as follows

$$R_5(t_n) = \int_0^\tau e^{(\tau-s)L}\Pi_N\Big[F'(\Pi_N\tilde{U}(t_n+s))$$
$$\cdot\int_0^s e^{(s-\sigma)L}\Pi_N\big[F(\Pi_N U(t_n+\sigma)) - F(\Pi_N\tilde{U}(t_n+\sigma))\big]d\sigma\Big]ds,$$

$$R_6(t_n) = \int_0^\tau e^{(\tau-s)L}\Pi_N\Big[F'(\Pi_N\tilde{U}(t_n+s))$$
$$\cdot\int_0^s \Big(e^{(s-\sigma)L}\Pi_N F(\Pi_N\tilde{U}(t_n+\sigma)) - e^{sL}\Pi_N F(\Pi_N U(t_n))\Big)d\sigma\Big]ds,$$

$$R_7(t_n) = \int_0^\tau se^{\tau L}\Pi_N\Big(e^{-sL}[F'(\Pi_N\tilde{U}(t_n+s))\cdot e^{sL}\Pi_N F(\Pi_N U(t_n))]$$
$$- F'(\Pi_N U(t_n))\Pi_N F(\Pi_N U(t_n))\Big)ds.$$

Finally, replacing $\Pi_N F$ by $I_N F$, we obtain

$$U(t_{n+1}) = e^{\tau L}U(t_n) + \tau e^{\tau L}I_N F(\Pi_N U(t_n))$$

9

$$+ (2L)^{-1} \left[\tau e^{\tau L} - (2L)^{-1} (e^{\tau L} - e^{-\tau L}) \right] H(\Pi_N U(t_n)) + \mathcal{L}^n, \qquad (4.11)$$

where $\mathcal{L}^n$ is the consistency error and is given by

$$\mathcal{L}^n = \sum_{i=1}^{9} R_i(t_n), \qquad (4.12)$$

$$R_8(t_n) = \tau e^{\tau L} (\Pi_N - I_N) F(\Pi_N U(t_n)), \qquad (4.13)$$

$$R_9(t_n) = (2L)^{-1} \left[\tau e^{\tau L} - (2L)^{-1} (e^{\tau L} - e^{-\tau L}) \right] \begin{pmatrix} -(\Pi_N - I_N) f(\Pi_N u(t_n)) \\ \Pi_N((I - I_N) f'(\Pi_N u(t_n)) \Pi_N v(t_n)) \end{pmatrix}. \qquad (4.14)$$

By dropping the remainder $\mathcal{L}^n$ and taking initial value $U_N^0 = \Pi_{N^\alpha} U(0)$, we obtain the following numerical scheme:

$$U_N^{n+1} = e^{\tau L} U_N^n + \tau e^{\tau L} I_N F(\Pi_N U_N^n) + (2L)^{-1} \left[\tau e^{\tau L} - (2L)^{-1} (e^{\tau L} - e^{-\tau L}) H(\Pi_N U_N^n) \right]. \qquad (4.15)$$

We recall the expression of $H(\Pi_N U_N^n)$ in (2.5) and apply the equality $\Pi_N I_N = I_N$. This yields the following algorithm for the low- and high-frequency parts of the numerical solution, respectively:

$$\Pi_N U_N^{n+1} = e^{\tau L} \Pi_N U_N^n + \tau e^{\tau L} I_N F(\Pi_N U_N^n)$$
$$+ (2L)^{-1} \left[\tau e^{\tau L} - (2L)^{-1} (e^{\tau L} - e^{-\tau L}) H(\Pi_N U_N^n) \right], \qquad (4.16)$$

$$\Pi_{(N, N^\alpha]} U_N^{n+1} = e^{\tau L} \Pi_{(N, N^\alpha]} U_N^n. \qquad (4.17)$$

This is algorithm (2.4), where (2.4c) is obtained by iterating (4.17) with respect to n.

The expressions of the remainders $R_j(t_n)$, $j = 1, \ldots, 9$, in this section are used in the error analysis in the next section.

5. Proof of Theorem 2.1 . Let $E_N^n = U(t_n) - U_N^n$ denote the error of the numerical solution and consider the difference between (4.11) and (4.15). This yields the following error equation:

$$E_N^{n+1} = e^{\tau L} E_N^n + \tau e^{\tau L} I_N \left(F(\Pi_N U(t_n)) - F(\Pi_N U_N^n) \right)$$
$$+ (2L)^{-1} \left[\tau e^{\tau L} - (2L)^{-1} \left(e^{\tau L} - e^{-\tau L} \right) \right] (H(\Pi_N U(t_n)) - H(\Pi_N U_N^n)) + \mathcal{L}^n, \quad (5.1)$$

with $E_N^0 = (I - \Pi_{N^\alpha}) U^0$. The remainder $\mathcal{L}^n$ in the expression above is estimated below.

PROPOSITION 5.1. *Under the conditions of Theorem 2.1, the remainder $\mathcal{L}^n$ in (5.1) satisfies the following estimates:*

$$\|\mathcal{L}^n\|_0 \lesssim \begin{cases} \tau N^{-\gamma+} + \tau^2 N^{1-2\gamma+} & \text{for} \quad \gamma \in (0, \frac{1}{2}] \\ \tau N^{-\gamma+} + \tau^2 N^{1-2\gamma+} + \min(\tau^2, \tau^3 N^{2(1-\gamma)+}) & \text{for} \quad \gamma \in (\frac{1}{2}, 1] \end{cases} \qquad (5.2)$$

and

$$\|\mathcal{L}^n\|_\gamma \lesssim \tau N^{-\gamma+} + \tau^2 N^{1-\gamma+}, \qquad (5.3)$$

where the constant is independent of τ.

Proof. In view of the definition $\mathcal{L}^n = \sum_{i=1}^{9} R_i(t_n)$, we present estimates for $R_j(t_n)$, $j = 1, \ldots, 9$, respectively.

ESTIMATE OF $R_1(t_n)$. We decompose $R_1(t_n)$ into the following parts:

$$R_1(t_n) = \int_0^\tau e^{(\tau - s)L} \Pi_{>N} F(\Pi_N U(t_n + s)) ds \qquad (5.4)$$

$$+ \int_0^\tau e^{(\tau - s)L} \left[F(U(t_n + s)) - F(\Pi_N U(t_n + s)) \right] ds. \qquad (5.5)$$

Lemma 3.1 (Bernstein's inequality) can be used to show that

$$\|(5.4)\|_1 \lesssim \tau N^{-\gamma} \max_{s \in [0, \tau]} \|F(\Pi_N U(t_n + s))\|_{1+\gamma} \lesssim \tau N^{-\gamma} \max_{s \in [0, \tau]} \|U(t_n + s)\|_\gamma.$$

10

By the mean-value theorem, we can rewrite (5.5) into the following expression:

$$(5.5) = \int_0^\tau e^{(\tau-s)L} \int_0^1 \left[F'\Big(\theta U(t_n+s) + (1-\theta)\Pi_N U(t_n+s)\Big) \cdot \Pi_{>N} U(t_n+s) \right] d\theta ds.$$

Then, according to (3.8) and Lemma 3.1, we obtain

$$\|(5.5)\|_1 \lesssim \tau \max_{s\in[0,\tau],\theta\in[0,1]} \|F'\left(\theta U(t_n+s) + (1-\theta)\Pi_N U(t_n+s)\right) \cdot \Pi_{>N} U(t_n+s)\|_1$$

$$= \tau \max_{s\in[0,\tau],\theta\in[0,1]} \|f'(\theta u(t_n+s) + (1-\theta)\Pi_N u(t_n+s)) \cdot \Pi_{>N} u(t_n+s)\|_{L^2}$$

$$\lesssim \tau \max_{s\in[0,\tau]} \|\Pi_{>N} u(t_n+s)\|_{L^2} \lesssim \tau N^{-\gamma} \max_{s\in[0,\tau]} \|U(t_n+s)\|_\gamma.$$

Therefore, by collecting the estimates (5.4) and (5.5), we have the following estimate of $\|R_1(t_n)\|_1$:

$$\|R_1(t_n)\|_1 \lesssim \tau N^{-\gamma} \max_{s\in[0,\tau]} \|U(t_n+s)\|_\gamma. \tag{5.6}$$

ESTIMATE OF $R_j(t_n)$ FOR $j = 2,\ldots,7$. Following the same discussions as in [35] (details can be found in [9]), one get

$$\|R_2(t_n)\|_1 + \|R_3(t_n)\|_1 \lesssim \tau^2 N^{-\gamma} + \tau^3, \tag{5.7}$$

$$\|R_4(t_n)\|_1 \lesssim \tau^2 N^{1-\gamma}, \tag{5.8}$$

$$\|R_4(t_n)\|_0 \lesssim \tau^3 N^{2(1-\gamma)+}, \tag{5.9}$$

$$\|R_5(t_n) + R_6(t_n) + R_7(t_n)\|_1 = \|I_2(t_n)\|_1 \lesssim \min(\tau^2, \tau^3 N^{2(1-\gamma)}). \tag{5.10}$$

On the other hand, we can also estimate $R_4(t_n)$ by using its following reformulated expression:

$$R_4(t_n) = \int_0^\tau e^{(\tau-2s)L}(\tau-s) \left[e^{2sL} G'(t_n+s) - G'(t_n) \right] ds, \tag{5.11}$$

with

$$G'(t_n+s) = \frac{d}{ds}\left(e^{-sL}\Pi_N F(\Pi_N \tilde{U}(t_n+s)) \right)$$

$$= e^{-sL}\begin{pmatrix} -\Pi_N f(\Pi_N \tilde{u}(t_n+s)) \\ \Pi_N\left(f'(\Pi_N \tilde{u}(t_n+s))\Pi_N \tilde{v}(t_n+s) \right) \end{pmatrix}, \tag{5.12}$$

by using (3.9) in Lemma 3.6, where $\tilde{U}(t_n+s) = e^{sL}U(t_n)$ is defined in (4.6). In this way, using the definition of G' in (5.12), we have

$$\|R_4(t_n)\|_0 \lesssim \tau^2 \sup_{s\in[0,\tau]} \|G'(t_n+s)\|_0$$

$$\lesssim \tau^2 \sup_{s\in[0,\tau]} \left(\|\Pi_N f(\Pi_N \tilde{u}(t_n+s))\|_{L^2} + \|\Pi_N\left(f'(\Pi_N \tilde{u}(t_n+s))\Pi_N \tilde{v}(t_n+s) \right)\|_{H^{-1}} \right).$$

According to (2.2), $\tilde{u}$ is bounded in L^2 and therefore the first term on the right-hand side above is $O(\tau^2)$. By employing Lemma 3.5, we can estimate the second term on the right-hand side above as follows:

$$\tau^2 \|\Pi_N\left(f'(\Pi_N \tilde{u}(t_n+s))\Pi_N \tilde{v}(t_n+s) \right)\|_{H^{-1}} \lesssim \begin{cases} \tau^2 N^{1-2\gamma+}\|U(t_n)\|_\gamma^2 & \text{for } \gamma \in (0, \tfrac{1}{2}] \\ \tau^2\|U(t_n)\|_\gamma^2 & \text{for } \gamma \in (\tfrac{1}{2}, 1]. \end{cases}$$

This, together with (5.9), yields the following estimate of $R_4(t_n)$ in the 0-norm:

$$\|R_4(t_n)\|_0 \lesssim \begin{cases} \tau^2 N^{1-2\gamma+}\|U(t_n)\|_\gamma^2 & \text{for } \gamma \in (0, \tfrac{1}{2}] \\ \min(\tau^2, \tau^3 N^{2(1-\gamma)+})\cdot\|U(t_n)\|_\gamma^2 & \text{for } \gamma \in (\tfrac{1}{2}, 1]. \end{cases} \tag{5.13}$$

ESTIMATE OF R_8 AND R_9: By using Lemma 3.1 and Lemma 3.2, we obtain

$$\|R_8\|_1 \lesssim \tau\|(\Pi_N - I_N)f(\Pi_N u(t_n))\|_{L^2} \lesssim \tau N^{-1-}\|f(\Pi_N u(t_n))\|_{H^{1+}} \lesssim \tau N^{-\gamma+}. \tag{5.14}$$

11

For $\|R_9\|_0$, by using (3.3), Lemma 3.1 and Lemma 3.2, we obtain

$$\|R_9\|_0 \lesssim \tau^2 \left(\|(\Pi_N - I_N)f(\Pi_N u(t_n))\|_{L^2} + \|(I - I_N)f'(\Pi_N u(t_n)) \cdot \Pi_N v(t_n)\|_{H^{-1}} \right)$$
$$\lesssim \tau^2 \left(N^{-1-}\|f(\Pi_N u(t_n))\|_{H^{1+}} + \|(I - I_N)f'(\Pi_N u(t_n))\|_{L^2}\|\Pi_N v(t_n)\|_{L^{2+}} \right)$$
$$\lesssim \tau^2 N^{-\gamma+} + \tau^2 N^{1-2\gamma+}. \tag{5.15}$$

For $\|R_9\|_\gamma$, according to (3.4), we derive

$$\|R_9\|_\gamma \lesssim \tau^2 \left(\|(\Pi_N - I_N)f(\Pi_N u(t_n))\|_{H^\gamma} + \|(I - I_N)f'(\Pi_N u(t_n))\Pi_n v(t_n)\|_{H^{\gamma-1}} \right)$$
$$\lesssim \tau^2 N^{-1+\gamma-}\|f(\Pi_N u(t_n))\|_{H^{1+}} + \tau^2\|(I - I_N)f'(\Pi_N u(t_n))\|_{L^2}\|\Pi_N v(t_n)\|_{H^{\gamma+}}$$
$$\lesssim \tau^2 N^{0+} + \tau^2 N^{1-\gamma+}\|v(t_n)\|_{H^{\gamma-1}}. \tag{5.16}$$

By summing up (5.6), (5.7), (5.13), (5.10), (5.14) and (5.15), we get the estimate (5.2) in the proposition 5.1. And combining (5.6), (5.7), (5.8), (5.10),(5.14) and (5.16) we finish the proof of (5.3) in the proposition 5.1. □

By using the estimates of the remainder in Proposition 5.1, Theorem 2.1 can be proved similarly as the error analysis in [35]. The details can be found in [9]. The proof of Theorem 2.2 (higher-order convergence rate in approximating discontinuous solutions with bounded variation) is more different from analysis in [35] and therefore presented below.

6. Proof of Theorem 2.2. From the estimates of the remainders in Section 5 we can see that $\|R_1(t_n)\|_0$ and $\|R_8(t_n)\|_0$ are $O(\tau N^{-\gamma+})$ while the other remainders are $O(\tau N^{-2\gamma+})$ under the step size condition $\tau \sim N^{-1}$. In the case $\gamma = \frac{1}{2}-$, all the remainders except $\|R_1(t_n)\|_0$ and $\|R_8(t_n)\|_0$ are $O(\tau^{2-})$, which leads to almost first-order convergence. Therefore, we only need to show the following improved error estimates for remainders $R_1(t_n)$ and $R_8(t_n)$ (see Lemma 6.1 and Lemma 6.2).

LEMMA 6.1. *Under the regularity condition $U \in C([0,T]; H^\gamma(\Omega) \times H^{\gamma-1}(\Omega))$ with $\gamma \in (0,1]$, the remainder $R_1(t_n)$ defined in (4.3) satisfies the following improved estimate:*

$$\max_{0 \le n \le M} \|R_1(t_n)\|_0 \lesssim \tau N^{-2\gamma+}. \tag{6.1}$$

Proof. We decompose $R_1(t_n)$ into the following two parts:

$$R_1(t_n) = \int_0^\tau e^{(\tau-s)L}\Pi_{>N}F(\Pi_N U(t_n + s))ds \tag{6.2}$$

$$+ \int_0^\tau e^{(\tau-s)L}\left[F(U(t_n + s)) - F(\Pi_N U(t_n + s))\right]ds, \tag{6.3}$$

where (6.3) can be further decomposed dyadically as follows (with $m = \lceil \log_2 N \rceil$ below):

$$(6.3) = \int_0^\tau e^{(\tau-s)L}\left[F(U(t_n + s)) - F(\Pi_{2^m N}U(t_n + s))\right]ds$$

$$+ \sum_{j=0}^{m-1}\int_0^\tau e^{(\tau-s)L}\left[F(\Pi_{2^{j+1}N}U(t_n + s)) - F(\Pi_{2^j N}U(t_n + s))\right]ds =: G_0 + \sum_{j=0}^{m-1}G_j.$$

By applying the mean-value theorem, we obtain

$$\|G_j\|_0 \lesssim \tau \sup_{s \in [0,\tau]}\|F(\Pi_{2^{j+1}N}U(t_n + s)) - F(\Pi_{2^j N}U(t_n + s))\|_0$$

$$\lesssim \tau \max_{s,\theta}\|f'(\xi) \cdot (\Pi_{2^{j+1}N} - \Pi_{2^j N})u(t_n + s)\|_{H^{-1}},$$

where $\xi = \theta\Pi_{2^{j+1}N}u(t_n + s) + (1 - \theta)\Pi_{2^j N}u(t_n + s)$. By estimating the last term above using (3.1), we have

$$\|G_j\|_0 \lesssim \tau\|(\Pi_{2^{j+1}N} - \Pi_{2^j N})u(t_n + s)\|_{H^{-1}}(\|f'(\xi)\|_{H^{1+}} + \|f'\|_{L^\infty})$$

$$\lesssim \tau(2^j N)^{-1-\gamma}\|u\|_{L^\infty H^\gamma}\left((2^j N)^{1-\gamma+}\|u\|_{L^\infty H^\gamma} + 1\right) \le \tau(2^j N)^{-2\gamma+}\|u\|_{L^\infty H^\gamma}^2.$$

12

For G_0, we have

$$\|G_0\|_1 \lesssim \tau \max_{s\in(0,\tau),\theta\in(0,1]} \|f'(\theta u(t_n+s) + (1-\theta)\Pi_{2^m N} u(t_n+s)) \cdot \Pi_{>2^m N} u(t_n+s)\|_{L^2}$$

$$\lesssim \tau \max_{s\in(0,\tau)} \|\Pi_{>N^2} u(t_n+s)\|_{L^2} \lesssim \tau N^{-2\gamma} \|u\|_{L^\infty H^\gamma}.$$

In summary, we have

$$\|(6.3)\|_0 \lesssim \tau N^{-2\gamma} + \sum_{j=0}^{m} \tau (2^j N)^{-2\gamma+} \lesssim \tau N^{-2\gamma+}. \tag{6.4}$$

On the other hand, Bernstein's inequality in Lemma 3.1 implies that

$$\|(6.2)\|_0 \lesssim \tau N^{-1-\gamma} \max_{s\in[0,\tau]} \|F(\Pi_N U(t_n+s))\|_{1+\gamma} \lesssim \tau N^{-1-\gamma} \|U\|_\gamma. \tag{6.5}$$

Therefore, by collecting (6.4) with (6.5), we obtain (6.1) for $\gamma \in (0,1]$. $\quad\square$

LEMMA 6.2. *Under the regularity condition* $U \in C([0,T]; H^{\frac{1}{2}-}(\Omega) \times H^{-\frac{1}{2}-}(\Omega))$ *and* $u \in L^\infty([0,T]; L^\infty(\Omega) \cap BV(\Omega))$, *the remainder term* $R_8(t_n)$ *defined in* (4.13) *satisfies the following estimate:*

$$\|R_8(t_n)\|_0 \lesssim \tau N^{-1+}, \quad \text{for each} \quad 0 \le n \le M. \tag{6.6}$$

Note that $R_8(t_n)$ is generated by the use of trigonometric interpolation I_N on the nonlinear function for the implementation of FFT. In order to prove Lemma 6.2, we need to use the following results for BV functions (see, for example [58, Section 5.3])

LEMMA 6.3. *For* $u \in BV(\Omega)$ *and* $\varepsilon > 0$, *we define* $u_\varepsilon = Eu * \varphi_\varepsilon$ *as the regularization of* u *based on an extension operator* $E : L^1(\Omega) \to L^1(\mathbb{R}^d)$ *which is bounded from* $W^{k,p}(\Omega)$ *to* $W^{k,p}(\mathbb{R}^d)$ *for all* $k \ge 0$ *and* $1 \le p \le \infty$, *and a mollifier* φ_ε *defined on* $\mathbb{R}^d$. *Then, for all sufficiently small* $\varepsilon > 0$,

$$\lim_{\varepsilon\to 0} \int_\Omega |u_\varepsilon - u| dx = 0, \tag{6.7}$$

$$\|u_\varepsilon\|_{BV(\Omega)} \lesssim \|u\|_{BV(\Omega)}. \tag{6.8}$$

Meanwhile, $u_\varepsilon \in C^\infty(\Omega)$ *and* $\|u_\varepsilon\|_{BV(\Omega)} = \|u_\varepsilon\|_{W^{1,1}(\Omega)}$, *and* $\|u_\varepsilon\|_{L^\infty(\Omega)} \le \|u\|_{L^\infty(\Omega)}$.

Proof of Lemma 6.2. By recalling the definition of $R_8(t_n)$ in (4.13) and applying the 0 norm, we obtain

$$\|R_8(t_n)\|_0 \lesssim \tau \|(\Pi_N - I_N) f(\Pi_N u(t_n))\|_{H^{-1}} \lesssim \tau \|(\Pi_N - I_N) f(\Pi_N u(t_n))\|_{L^{1+}}. \tag{6.9}$$

In one dimension, we obtain the following estimate by using Lemma 3.1 and Lemma 3.3:

$$\|R_8(t_n)\|_0 \lesssim \tau \|(\Pi_N - I_N) f(\Pi_N u_\varepsilon(t_n))\|_{L^{1+}} + \tau \|(\Pi_N - I_N)\left[f(\Pi_N u(t_n)) - f(\Pi_N u_\varepsilon(t_n))\right]\|_{L^{1+}}$$

$$\lesssim \tau N^{-1} \|f(\Pi_N u_\varepsilon(t_n))\|_{W^{1,1+}} + \tau N^{-1} \|f(\Pi_N u(t_n)) - f(\Pi_N u_\varepsilon(t_n))\|_{W^{1,1+}}. \tag{6.10}$$

The first term in the right hand side of (6.10) can be estimated by using the Lipschitz continuity of f and the Sobolev embedding, i.e.,

$$\tau N^{-1} \|f(\Pi_N u_\varepsilon(t_n))\|_{W^{1,1+}} \lesssim \tau N^{-1} \|\Pi_N u_\varepsilon(t_n)\|_{W^{1,1+}} \lesssim \tau N^{-1+} \|u_\varepsilon(t_n)\|_{W^{1-,1+}}$$

$$\lesssim \tau N^{-1+} \|u_\varepsilon(t_n)\|_{W^{1,1}}$$

$$= \tau N^{-1+} \|u_\varepsilon(t_n)\|_{BV}.$$

The second term in the right hand side of (6.10) can be estimated as follows:

$$\tau N^{-1} \|f(\Pi_N u(t_n)) - f(\Pi_N u_\varepsilon(t_n))\|_{W^{1,1+}} \le \tau N^{-1} \|f(\Pi_N u(t_n)) - f(\Pi_N u_\varepsilon(t_n))\|_{L^{1+}}$$

$$+ \tau N^{-1} \|\nabla \Pi_N u(t_n)\left(f'(\Pi_N u(t_n)) - f'(\Pi_N u_\varepsilon(t_n))\right)\|_{L^{1+}}$$

$$+ \tau N^{-1} \|f'(\Pi_N u_\varepsilon(t_n))\left(\nabla \Pi_N u(t_n) - \nabla \Pi_N u_\varepsilon^n\right)\|_{L^{1+}}$$

$$\lesssim \tau N^{\frac{1}{2}+} \|u(t_n) - u_\varepsilon(t_n)\|_{L^{1+}}.$$

13

where the last inequality uses the Lipschitz condition of f and the following result:

$$\tau N^{-1}\|\nabla\Pi_N u(t_n)\left(f'(\Pi_N u(t_n)) - f'(\Pi_N u_\varepsilon(t_n))\right)\|_{L^{1+}}$$

$$\lesssim \tau N^{-1}\|\nabla\Pi_N u(t_n)\|_{L^\infty}\|f'(\Pi_N u(t_n)) - f'(\Pi_N u_\varepsilon(t_n))\|_{L^{1+}}$$

$$\lesssim \tau N^{\frac{1}{2}+}\|u(t_n)\|_{H^{\frac{1}{2}-}}\|u(t_n) - u_\varepsilon(t_n)\|_{L^{1+}}.$$

Combining these estimates, we have

$$\|R_8(t_n)\|_0 \lesssim \tau N^{-1+}\|u_\varepsilon(t_n)\|_{BV} + \tau N^{\frac{1}{2}+}\|u(t_n) - u_\varepsilon(t_n)\|_{L^{1+}}. \tag{6.11}$$

Under the assumption $u \in L^\infty([0,T]; L^\infty(\Omega))$, since $\|u_\varepsilon\|_{L^\infty}$ is uniformly bounded by $\|u\|_{L^\infty}$ and, according to (6.7),

$$\|u(t_n) - u_\varepsilon(t_n)\|_{L^{1+}} \le \|u(t_n) - u_\varepsilon(t_n)\|_{L^\infty}^{0+}\|u(t_n) - u_\varepsilon(t_n)\|_{L^1}^{1-} \to 0 \quad \text{as } \varepsilon \to 0.$$

Thus, for any fixed N, we can choose $\varepsilon \ll 1$ such that $\tau N^{\frac{1}{2}+}\|u(t_n) - u_\varepsilon(t_n)\|_{L^{1+}} \lesssim \tau N^{-1+}$. This, together with (6.8) and (6.11), yields (6.6). This proves Lemma 6.2. □

Under the conditions of Theorem 2.2 (with $\gamma = \frac{1}{2}-$), Lemma 6.1 and Lemma 6.2 imply that $\|R_1(t_n)\|_0$ and $\|R_8(t_n)\|_0$ are both $O(\tau^{2-})$ under the step size condition $\tau \sim N^{-1}$, and the other remainders in the $\|\cdot\|_0$ norm have been shown to be $O(\tau^{2-})$ in Section 5. Therefore, the following result holds:

$$\|\mathcal{L}^n\|_0 \lesssim \tau^{2-}. \tag{6.12}$$

By using the estimate of the remainder in (6.12), the following error estimate can be proved for the low-frequency and high-frequency parts, respectively (details can be found in [9]):

$$\|\Pi_N(U(t_{n+1}) - U_N^{n+1})\|_0 \le C\Big[\|\Pi_N(U(0) - U_N^0)\|_0$$

$$+ \sum_{j=0}^n \Big(\tau\|\Pi_N(U(t_j) - U_N^j)\|_0 + \|\Pi_N\mathcal{L}^j\|_0 + \tau^{2-}\Big)\Big], \tag{6.13}$$

$$\|\Pi_{(N,N^2]}(U(t_{n+1}) - U_N^{n+1})\|_0 \le C\Big(\|\Pi_{(N,N^2]}(U(0) - U_N^0)\|_0 + \sum_{j=0}^n \|\Pi_{(N,N^2]}\mathcal{L}^j\|_0\Big). \tag{6.14}$$

Since our choice of initial value $U_N^0 = \Pi_{N^2}U(0)$ implies that

$$\|\Pi_N(U(0) - U_N^0)\|_0 = \|\Pi_{(N,N^2]}(U(0) - U_N^0)\|_0 = 0,$$

by using the improved estimate on $\|\mathcal{L}^j\|_0$ in (6.12) and Gronwall's inequality, we obtain the following result from (6.13)–(6.14):

$$\|\Pi_{N^2}U(t_{n+1}) - U_N^{n+1}\|_0 \le C\tau^{1-}. \tag{6.15}$$

This, together with an estimate of the projection error $\|U(t_{n+1}) - \Pi_{N^2}U(t_{n+1})\|_0$ for $U^0 \in H^{\frac{1}{2}-}(\Omega) \times H^{-\frac{1}{2}-}(\Omega)$, leads to the error estimate in Theorem 2.2. □

From the proof of Theorem 2.2 we see that, without introducing the high-frequency recovery, the numerical solution still satisfies $\|\Pi_N U(t_{n+1}) - U_N^{n+1}\|_0 \le C\tau^{1-}$ but only satisfies $\|U(t_{n+1}) - U_N^{n+1}\|_0 \le C\tau^{\frac{1}{2}-}$. This reduction of convergence rate (when there is no high-frequency recovery) can be observed in the numerical tests.

7. Numerical examples. In this section, we present extensive numerical examples to support the theoretical analysis and to illustrate the effectiveness of the low-regularity integrator in this paper in capturing the interface of discontinuity in the solutions, as well as the accuracy (without spurious oscillations) in approximating rough and discontinuous solutions of the semilinear wave equation.

7.1. The Sine–Gordon equation in one dimension. We consider the semilinear wave equation in (1.1) with a nonlinear function $g(u) = 40\sin(u)$ for the following piecewise

14

smooth discontinuous initial state:

$$\big(u^0(x), v^0(x)\big) = \begin{cases} (5, -5), & \text{for } x \in \big[0.3, 0.425\big], \\ (2.5, -2.5), & \text{for } x \in \big[0.575, 0.7\big], \\ (0, 0), & \text{else where,} \end{cases} \tag{7.1}$$

which satisfies the conditions of Theorem 2.2. As a result, the low-regularity integrator `HR-LRI` in (2.4) with $\alpha = 2$ should have almost first-order convergence by choosing $N = O(\tau^{-1})$. We solve the problem with $N = 2^{10}$ and $4\tau = N^{-1}$, and present the evolution of the numerical solution for $t \in [0, T]$ in Figure 7.1 (a), which clearly shows the propagation of discontinuities of the solution.
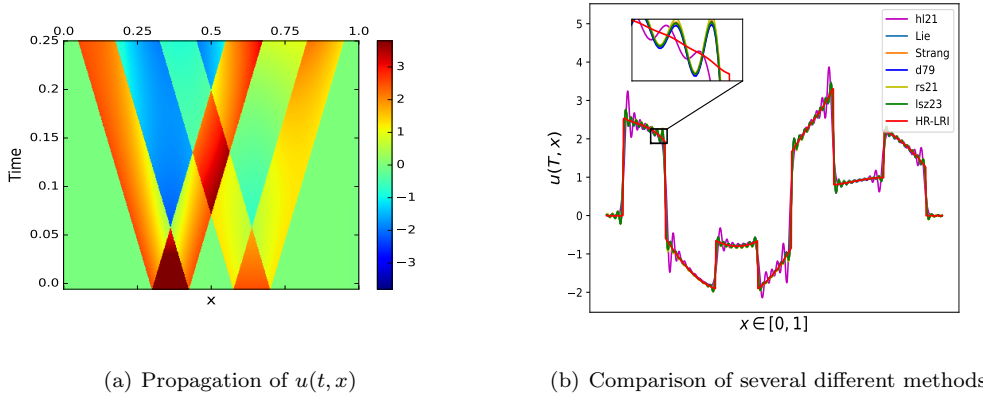

(a) Propagation of $u(t, x)$

(b) Comparison of several different methods

FIG. 7.1. *Numerical solution of the 1D problem with discontinuous initial value in* (7.1).

(a) $L^2(\Omega) \times H^{-1}(\Omega)$ error versus τ

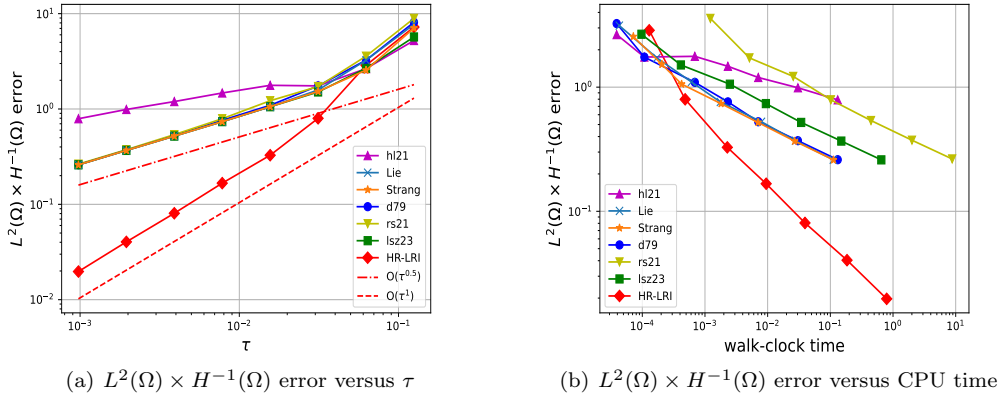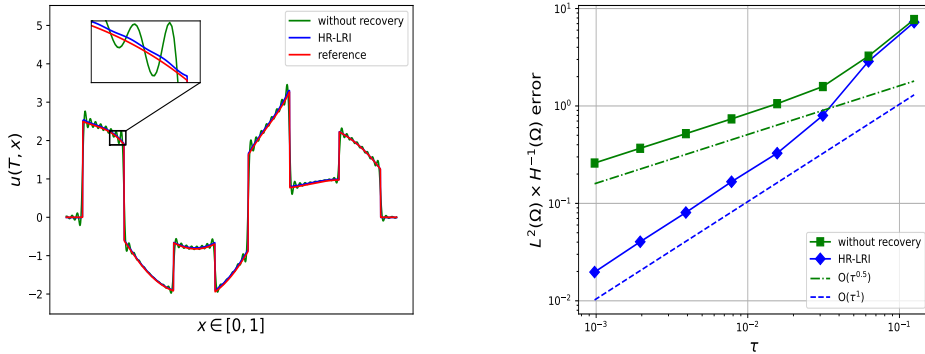(b) $L^2(\Omega) \times H^{-1}(\Omega)$ error versus CPU time

FIG. 7.2. *Comparison of numerical solutions given by several different methods.*

In Figure 7.1 (b), we plot the numerical solutions at time T computed by several different numerical methods, including the second-order low-regularity correction of Lie splitting method from [38] (which is referred to as `lsz23`), the second-order low-regularity exponential-type scheme from [48] (which is referred to as `rs21`), the second-order IMEX method from [27] (referred to as `hl21`), the second-order trigonometric integrators constructed by Deuflhard [15] (referred to as `d79`), and classical splitting methods such as the Lie splitting scheme and Strang splitting scheme. The time step sizes and number of

Fourier modes in all these methods are chosen to be $\tau = N^{-1}/4$ and $N = 2^7$, respectively. From the numerical results in Figure 7.1 (b) we can see that the discontinuities in the exact solution may lead to significant oscillations in the solutions of the pre-existing methods, while the proposed method in `HR-LRI` can substantially reduce the numerical oscillations with equivalent computational cost.

In Theorem 2.2 and Remark 2.5 we have shown that, since the initial value of the solution is in $BV(\Omega) \cap L^\infty(\Omega)$, the error of the numerical solution is $O(\tau^{1-})$. In Figure 7.2 we compare the $L^2(\Omega) \times H^{-1}(\Omega)$ errors of the numerical solutions at $T = 0.25$ computed by the several different methods with step size $\tau = N^{-1}/4$ and the reference solutions are given by the proposed method with a sufficiently large $N = 2^{14}$. The numerical results Figure 7.2 are consistent with the theoretical results proved in Theorem 2.2 and demonstrates that the proposed method has a higher convergence rate (with respect to both step size and CPU time) than pre-existing methods in approximating discontinuous solutions of the semilinear wave equations.

To further demonstrate the effectiveness of the proposed high-frequency recovery process, we compare the numerical solutions before and after high-frequency recovery at time $T = 0.25$ in Figure 7.3 (a). Here, `HR-LRI` represents the high-frequency recovery algorithm proposed in this paper, with $N = 2^7$, $\tau = N^{-1}/4$, and $\alpha = 2$. The "`Without recovery`" corresponds to the algorithm (2.4) without undergoing the high-frequency recovery process, with $N = 2^7$ and $\tau = N^{-1}/4$. The reference solution in Figure 7.3 (a) is obtained by using the proposed algorithm with sufficiently large $N = 2^{14}$. And, in Figure 7.3 (b), we compare the errors of numerical solutions before and after high-frequency recovery under the condition $\tau = N^{-1}/4$. As rigorously proved by Theorem 2.2, the numerical experiments show that the high-frequency recovery process significantly reduces the oscillations of the solution, resulting in a higher order of convergence accuracy, whereas in the absence of the high-frequency recovery process, the numerical algorithm's order of convergence decreases significantly.

(a) Comparison before and after high-frequency recovery process

(b) $L^2(\Omega) \times H^{-1}(\Omega)$ error versus τ

FIG. 7.3. *Numerical results of the 1D problem with the initial value in* (7.1).

7.2. The Sine–Gordon equation in two dimensions.
In this section, we consider the semilinear wave equation with $g(u) = 4\sin(u)$ for the initial states:

(i) Propagation of one discontinuous wave:

$$\left(u^0(x), v^0(x)\right) = \begin{cases} (0.5, 0), & \text{for } x \in \left[0.375, 0.625\right]^2, \\ (0, 0), & \text{else where.} \end{cases}$$

16

(ii) Propagation of two discontinuous waves:

$$\left(u^0(x), v^0(x)\right) = \begin{cases} (0.5, 0), & \text{for } x \in \left[0.3, 0.425\right]^2, \\ (0.25, 0), & \text{for } x \in \left[0.575, 0.7\right]^2, \\ (0, 0), & \text{else where.} \end{cases}$$

(iii) A rough initial value in $H^{\frac{1}{2}} \times H^{-\frac{1}{2}}$:

$$(u^0(x), v^0(x)) = \Big(\frac{1}{C_u} \sum_{k,l \in \mathbb{Z}} a_u(k) b_u(l) e^{i(kx_1 + lx_2)}, \ \frac{1}{C_v} \sum_{k,l \in \mathbb{Z}} a_v(k) b_v(l) e^{i(kx_1 + lx_2)}\Big),$$

(7.2)

where

$$\begin{cases} a_u(k) = \text{rand}(0, 1)|k|^{-1.01}, & b_u(l) = \text{rand}(0, 1)|l|^{-1.01}, \\ a_v(k) = \text{rand}(0, 1)|k|^{-0.01}, & b_v(l) = \text{rand}(0, 1)|l|^{-0.01}, \end{cases}$$

and C_u and C_v are constants such that $\|u^0\|_{H^{\frac{1}{2}}} = \|v^0\|_{H^{-\frac{1}{2}}} = 1$.

We solve the semilinear wave equation by the Strang splitting method and the proposed low-regularity integrator `HR-LRI` in (2.4) with $\alpha = \frac{3}{2}$ for the initial values in (i) and (ii), and plot the numerical solutions in Figure 7.4–7.5 by choosing $\tau = N^{-1}/4 = 2^{-8}$. The results show that the proposed method can effectively eliminate the high oscillation of numerical solutions in approximating discontinuous solutions of the semilinear wave equation.
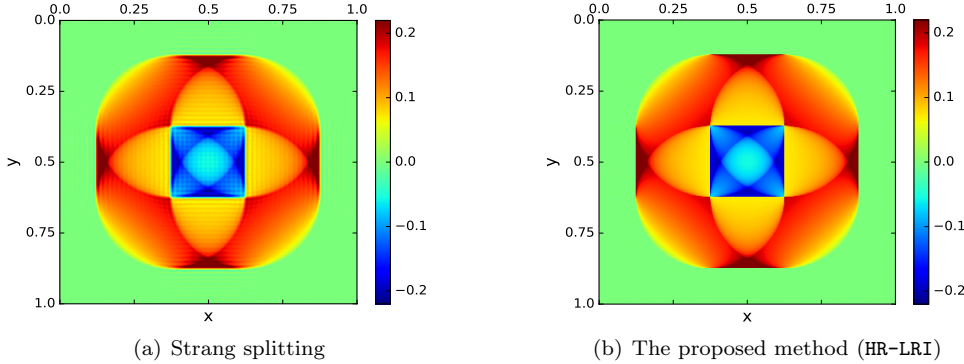

(a) Strang splitting   (b) The proposed method (`HR-LRI`)

FIG. 7.4. *Comparison of the numerical solutions at $t = 0.25$ computed by two different methods*

(a) Strang splitting   (b) The proposed method (`HR-LRI`)

FIG. 7.5. *Comparison of the numerical solutions at $t = 0.25$ computed by two different methods*

17

(a) Error vs τ for initial state (i)

(b) Error vs CPU time for initial state (i)

(c) Error vs τ for initial state (iii)

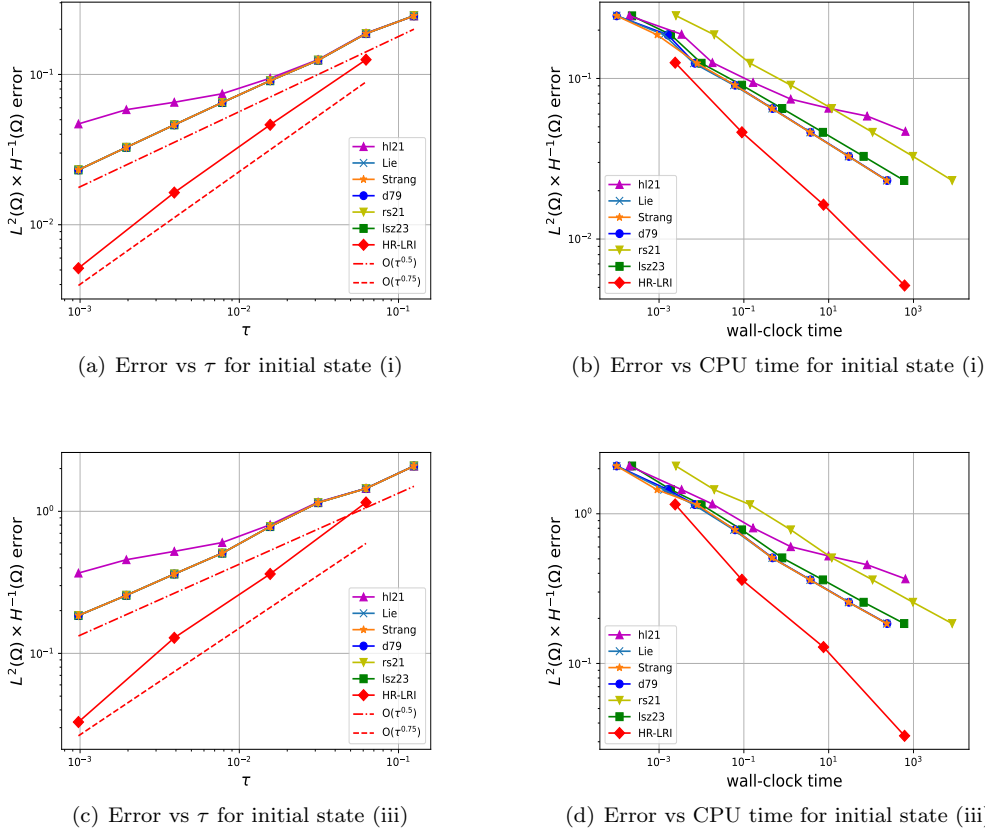(d) Error vs CPU time for initial state (iii)
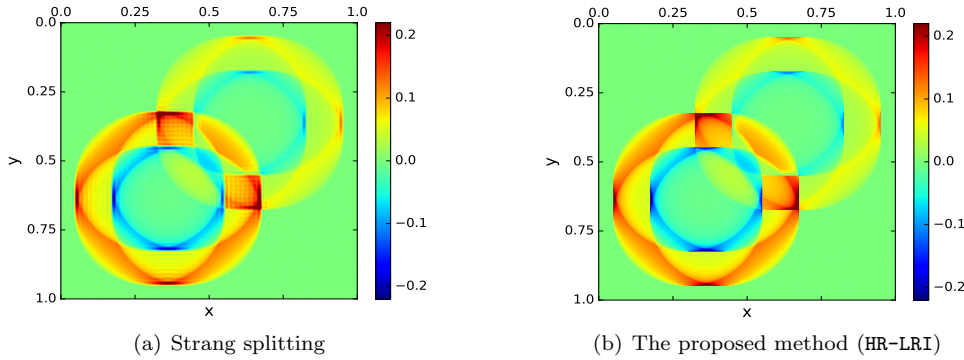
FIG. 7.6. *Comparison of numerical solutions given by several different methods in two dimensional cases.*

The errors of the numerical solutions computed by several different numerical methods are presented in Figure 7.6 with $4\tau = N^{-1}$, where the reference solution is given by the proposed method with sufficiently large N and sufficiently small τ. The numerical results in Figure 7.6 are again consistent with the theoretical results proved in Theorem 2.1, i.e., the proposed method has convergence order $\frac{3}{4}$ while the other methods have convergence order $\frac{1}{2}$ or smaller. The convergence rate of the proposed method with respect to CPU time is also faster than pre-existing methods in approximating the discontinuous solution of the two-dimensional semilinear wave equation.

7.3. The Klein–Gordon equation in one dimension. In the last example, we consider the one-dimensional Klein–Gordon equation with a locally Lipschitz continuous (not globally Lipschitz continuous) nonlinear function $g(u) = u^3$, with the following piecewise smooth discontinuous initial state:

$$\left(u^0(x), v^0(x)\right) = \begin{cases} (4, 0), & \text{for } x \in \left[0.3, 0.425\right], \\ (2, 0), & \text{for } x \in \left[0.575, 0.7\right], \\ (0, 0), & \text{else where,} \end{cases} \tag{7.3}$$

which leads to a bounded piecewise smooth discontinuous solution. Since the Lipschitz continuity condition (2.6) can be satisfied when $u(t, x)$ is uniformly bounded for $(t, x) \in [0, T] \times \Omega$, the theoretical results in Theorem 2.1 and Theorem 2.2 are also applicable to
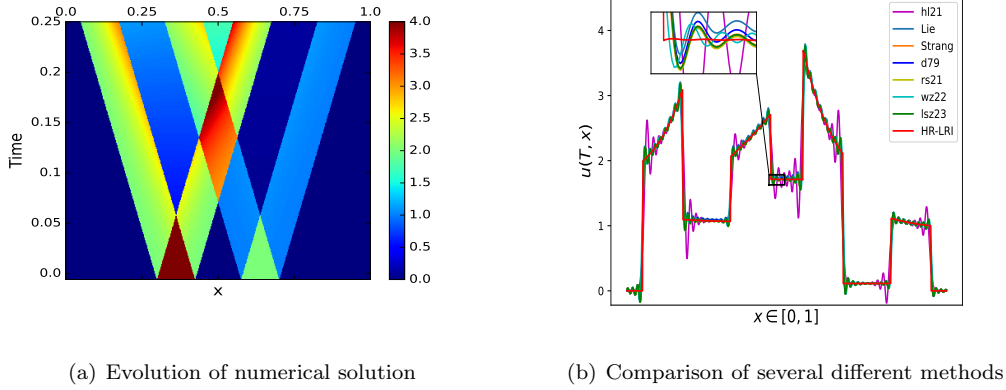
this problem.

(a) Evolution of numerical solution

(b) Comparison of several different methods

Fig. 7.7. *Numerical solution with the initial value in* (7.3).

(a) $L^2(\Omega) \times H^{-1}(\Omega)$ error versus τ

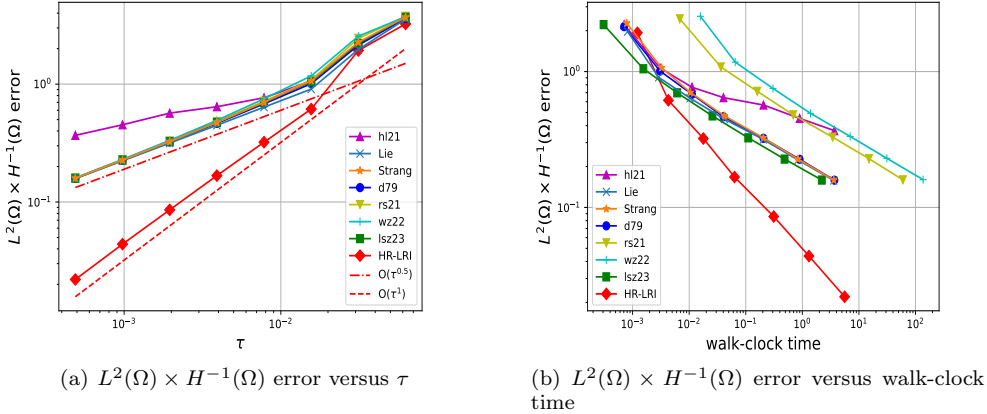(b) $L^2(\Omega) \times H^{-1}(\Omega)$ error versus walk-clock time

Fig. 7.8. *Errors of the numerical solutions with the initial value in* (7.3).

We solve the Klein–Gordon equation with $\tau = N^{-1}/4 = 2^{-12}$ and present the evolution of the numerical solution in Figure 7.7 (a), which shows the propagation of discontinuities of the solution. In Figure 7.7 (b) we compare the numerical solutions at $T = 0.25$ computed by several different methods. Here the symmetric low-regularity integrator for semilinear Klein–Gordon equation in [53] is also taken into comparison and referred to as wz22. The numerical results in Figure 7.7 (b) indicate that the proposed method indeed improves the accuracy and reduces spurious oscillations.

In addition, we present the errors of the numerical solutions computed by the several different methods in Figure 7.8, which shows that the proposed method has first-order convergence with respect to the step size τ in approximating such discontinuous solutions, and the usual methods have half-order convergence in this case. This is consistent with the convergence rate proved in Theorem 2.2 and demonstrates the efficiency of the proposed method in approximating rough and discontinuous solutions.

REFERENCES

[1] Genming Bai, Buyang Li, and Yifei Wu: A constructive low-regularity integrator for the 1d cubic nonlinear Schrödinger equation under the Neumann boundary condition. *IMA J. Numer. Anal.* (2022) DOI: 10.1093/imanum/drac075

[2] Weizhu Bao, Yue Feng, and Chunmei Su: Uniform error bounds of time-splitting spectral methods for the long-time dynamics of the nonlinear wave equation with weak nonlinearity. *Math. Comp.* 91 (2022), pp. 811–842.

[3] Weizhu Bao and Li Yang: Efficient and accurate numerical methods for the Klein–Gordon–Schrödinger equations. *J. Comput. Phys.* 225 (2007), pp. 1863–1893.

[4] A. Barone, F. Esposito, C. J. Magee: Theory and applications of the sine-gordon equation. *La Rivista del Nuovo Cimento* 1 (1971), pp. 227–267 (1971).

[5] Jean Bourgain, *Global Solutions of Nonlinear Schr ̈odinger Equations*, American Mathematical Society Colloquium Publications, vol. 46, American Mathematical Society, Providence, RI, 1999.

[6] Yvain Bruned and Katharina Schratz: Resonance based schemes for dispersive equations via decorated trees. To appear in *Forum of Mathematics, Pi*, 10, E2. DOI:10.1017/fmp.2021.13

[7] Simone Buchholz, Benjamin Dörich, and Marlis Hochbruck: On averaged exponential integrators for semilinear wave equations with solutions of low-regularity. *SN Partial Differ. Equ. Appl.* 2 (2021), pp. 2662–2963.

[8] Jiachuan Cao, Buyang Li, and Yanping Lin: A new second-order low-regularity integrator for the cubic nonlinear Schrödinger equation. *IMA J. Numer. Anal.* (2023) DOI: 10.1093/imanum/drad017

[9] Jiachuan Cao, Buyang Li, Yanping Lin, and Fangyan Yao: Numerical approximation of discontinuous solutions of the semilinear wave equation (arXiv version of the current paper), arXiv:2312.10392

[10] Waixiang Cao, Dongfang Li, and Zhimin Zhang: Unconditionally optimal convergence of an energy-conserving and linearly implicit scheme for nonlinear wave equations. *Sci. China Math.* (2021). https://doi.org/10.1007/s11425-020-1857-5

[11] Chuchu Chen, Jialin Hong, Chol Sim, and Kwang Sonwu: Energy and quadratic invariants preserving (EQUIP) multi-symplectic methods for Hamiltonian wave equations. *J. Comput. Phys.* 418 (2020), article 10959.

[12] David Cohen, Ernst Hairer, and Christian Lubich. Conservation of energy, momentum and actions in numerical discretizations of non-linear wave equations. *Numer. Math.* 110 (2008), pp. 113–143.

[13] Jesús Cuevas-Maraver, Panayotis G. Kevrekidis, and Floyd Williams, *The sine-Gordon model and its applications*, Nonlinear systems and complexity 10 (2014).

[14] Aleksandr S. Davydov, *Quantum mechanics: international series in natural philosophy.* Vol. 1. Elsevier, 2013.

[15] Peter Deuflhard: A study of extrapolation methods based on multistep schemes without parasitic solutions. *Z. Angew. Math. Phys.* 30 (1979), pp. 177–189.

[16] Eskil Hansen and Alexander Ostermann: High-order splitting schemes for semilinear evolution equations. *BIT Numer. Math.* 56 (2016), pp. , 1303–1316.

[17] Ludwig Gauckler: Error analysis of trigonometric integrators for semilinear wave equations. *SIAM J. Numer. Anal.* 53, 2, (2015), pp. 1082-1106.

[18] Bosco García-Archilla, Jesús María Sanz-Serna, and Robert D. Skeel: Long-time-step methods for oscillatory differential equations. *SIAM J. Sci. Comput.* 20 (1998), pp. 930-963.

[19] Jean Ginibre and Ginibre Velo, The global Cauchy problem for the nonlinear Klein-Gordon equation, *Math. Z.* 189 (1985), no. 4, pp. 487–505.

[20] Jean Ginibre and Ginibre Velo, The global Cauchy problem for the nonlinear Klein-Gordon equation II (English, with French summary), *Ann. Inst. H. Poincaré Anal. Non Linéaire* 6 (1989), no. 1, pp. 15–35.

[21] Roland Glowinski and Annalisa Quaini: On the numerical solution to a nonlinear wave equation associated with the first Painlevé equation: an operator-splitting approach. *Partial Differential Equations: Theory, Control and Approximation*, pp. 243–264, Springer, Dordrecht, 2014.

[22] Volker Grimm and Marlis Hochbruck: Error analysis of exponential integrators for oscillatory second-order differential equations. *J. Phys. A* 39 (2006), pp. 5495–5507.

[23] A.M. Grundland and Eryk Infeld: A family of nonlinear Klein-Gordon equations and their solutions. *J. Math. Phys.* 33 (1992), pp. 2498–2503.

[24] B. Guo: Spectral Methods and Their Applications. World Scientific (1998).

[25] Ernst Hairer and Christian Lubich: Long-time energy conservation of numerical methods for oscillatory differential equations. *SIAM J. Numer. Anal.* 38 (2000), pp. 414–441.

[26] Ernst Hairer, Christian Lubich, and Gerhard Wanner: *Geometric Numerical Integration. Structure-Preserving Algorithms for Ordinary Differential Equations*. Second Edition. Springer 2006.

[27] Marlis Hochbruck and Jan Leibold: An implicit-explicit time discretization scheme for second-order semilinear wave equations with application to dynamic boundary conditions. *Numer. Math.* 147 (2021), pp. 869–899.

[28] Marlis Hochbruck and Christian Lubich: A Gautschi-type method for oscillatory second-order differ-

ential equations. *Numer. Math.* 83 (1999), pp. 403–426.

[29] Martina Hofmanová and Katharina Schratz: An exponential-type integrator for the KdV equation. *Numer. Math.* 136 (2017), pp. 1117–1137.

[30] Vladimir H. Hristov: Best onesided approximation and mean approximation by interpolation polynomials of periodic functions. *Math. Balkanica*, New Series 3: Fasc. 3–4.

[31] Frederick W. King, Hilbert Transforms, Cambridge University Press, New York, 2009.

[32] Rainer Kress, *Linear Integral Equations*, Springer, New York, 1989.

[33] William Layton, Yong Li, and Catalin Trenchea: Recent developments in IMEX methods with time filters for systems of evolution equations. *J. Comput. Appl. Math.* 299 (2016), pp. 50–67.

[34] Buyang Li, Shu Ma, and Katharina Schratz: A semi-implicit low-regularity integrator for Navier–Stokes equations. *SIAM J. Numer. Anal.* 60 (2022), pp. 2273–2292.

[35] Buyang Li, Katharina Schratz, and Franco Zivcovich: A second-order low-regularity correction of Lie splitting for the semilinear wave equation. To appear in ESAIM:M2AN.

[36] Buyang Li and Yifei Wu, A full discrete low-regularity integrator for the 1D period cubic nonlinear Schrödinger equation, *Numer. Math.* 149 (2021), pp. 151–183.

[37] Dongfang Li and Weiwei Sun: Linearly implicit and high-order energy-conserving schemes for nonlinear wave equations. *J. Sci. Comput.* 83 (2020), article 65.

[38] Dong Li and Yannick Sire: Remarks on the Bernstein inequality for higher order operators and related results. Transactions of the American Mathematical Society 376 (2023), pp. 945–967.

[39] Jichun Li and Miguel R. Visbal: High-order compact schemes for nonlinear dispersive waves. *J. Sci. Comput.* 26 (2006), pp. 1–23.

[40] D. Murai and T. Koto: Stability and convergence of staggered Runge–Kutta schemes for semilinear wave equations. J. Comput. Appl. Math. 235 (2011), pp. 4251–4264.

[41] Alexander Ostermann and Katharina Schratz: Low regularity exponential-type integrators for semilinear Schrödinger equations. *Found. Comput. Math.* 18 (2018), pp. 731–755.

[42] Alexander Ostermann, Frédéric Rousset, and Katharina Schratz: Fourier integrator for periodic NLS: low regularity estimates via discrete Bourgain spaces. To appear in *J. Eur. Math. Soc.*

[43] Alexander Ostermann, Frédéric Rousset, and Katharina Schratz: Error estimates at low regularity of splitting schemes for NLS *Math. Comp.* 91 (2022), pp.169–182.

[44] Alexander Ostermann and Fangyan Yao: A fully discrete low-regularity integrator for the nonlinear Schrödinger equation. J. Sci. Comput. 91 (2022).

[45] Ruisheng Qi and Xiaojie Wang: Error estimates of finite element method for semilinear stochastic strongly damped wave equation. *IMA J. Numer. Anal.* 39 (2019) 39, pp. 1594–1626.

[46] Annalisa Quaini and Roland Glowinski: Splitting methods for some nonlinear wave problems. *Splitting Methods In Communication, Imaging, Science, and Engineering*, pp. 643–676, Scientific Computation Series, Springer, Cham, 2016.

[47] Jürgen Prestin and Yuan Xu: Convergence rate for trigonometric interpolation of non-smooth functions, *J. Approx. Theory*, 77 (2) (1994), pp. 113–122.

[48] Frédéric Rousset and Katharina Schratz: A general framework of low-regularity integrators. *SIAM J. Numer. Anal.* 59 (2021), pp. 1735–1768.

[49] Zhijian Rong and Chuanju Xu: Numerical approximation of acoustic waves by spectral element methods. *Appl. Numer. Math.* 58 (2008), pp. 999–1016.

[50] Gilbert Strang: On the construction and comparison of difference schemes. *SIAM J. Numer. Anal.* 5.3 (1968), pp. 506-517.

[51] Bin Wang and Xinyuan Wu: The formulation and analysis of energy-preserving schemes for solving high-dimensional nonlinear wave equations. *IMA J. Numer. Anal.* 39 (2019), pp. 2016–2044.

[52] Bin Wang and Xinyuan Wu: Global error bounds of one-stage extended RKN integrators for semilinear wave equations. *Numer. Algorithm* 81 (2019), pp. 1203–1218.

[53] Yan Wang and Xiaofei Zhao: A symmetric low-regularity integrator for nonlinear wave equation. *Math. Comp.* 91 (2022), pp. 2215–2245.

[54] Yongsheng Li, Yifei Wu, and Fangyan Yao: Convergence of an embedded exponential-type low-regularity integrators for the KdV equation without loss of regularity. *Ann. Appl. Math.* 37 (2021), pp. 1–21.

[55] Yifei Wu and Fangyan Yao: A first-order Fourier integrator for the nonlinear Schrödinger equation. *Math. Comput.* 91 (2021), pp. 1213–1235.

[56] Yifei Wu and Xiaofei Zhao: Optimal convergence of a first order low-regularity integrator for the KdV equation. *IMA J. Numer. Anal.* (2021), DOI: 10.1093/imanum/drab054

[57] Yifei Wu and Xiaofei Zhao: Embedded exponential-type low-regularity integrators for KdV equation under rough data. *BIT Numer. Math.* 62 (2022), pp. 1049–1090.

[58] William P. Ziemer: *Weakly differentiable functions: Sobolev spaces and functions of bounded variation.* Vol. 120. Springer Science & Business Media, 2012.